

Title: Correlation of ⁶⁸Ga-RM2 PET with Post-Surgery Histopathology Findings in Patients with Newly Diagnosed Intermediate- or High-Risk Prostate Cancer

Authors: Heying Duan¹, Lucia Baratto¹, Richard E. Fan², Simon John Christoph Soerensen^{2,3}, Tie Liang¹, Benjamin Inbeh Chung², Alan Eih Chih Thong², Harcharan Gill², Christian Kunder⁴, Tanya Stoyanova⁵, Mirabela Rusu⁶, Andreas M. Loening⁷, Pejman Ghanouni⁷, Guido A. Davidzon¹, Farshad Moradi¹, Geoffrey A. Sonn², Andrei Iagaru¹

Author Affiliations:

¹ Department of Radiology, Division of Nuclear Medicine and Molecular Imaging, Stanford University, Stanford, CA, USA

² Department of Urology, Stanford University, Stanford, CA, USA

³ Department of Epidemiology and Population Health, Stanford University, Stanford, CA, USA

⁴ Department of Pathology, Stanford University, Stanford, CA, USA

⁵ Radiology, Canary Center at Stanford for Cancer Early Detection, Stanford University, Stanford, CA, USA

⁶ Department of Radiology, Division of Integrative Biomedical Imaging, Stanford University, Stanford, CA, USA

⁷ Department of Radiology, Division of Body MRI, Stanford University, Stanford, CA, USA

First author:

Heying Duan, MD (Research fellow), ORCID 0000-0002-2834-5524

Department of Radiology, Division of Nuclear Medicine and Molecular Imaging
Stanford University

300 Pasteur Drive, H2200

Stanford, CA 94305, USA

Phone: +1 650 725 4711

Fax: +1 650 498 5047

heyings@stanford.edu

Corresponding author:

Andrei Iagaru, MD, ORCID 0000-0003-0839-5329

Department of Radiology, Division of Nuclear Medicine and Molecular Imaging

Stanford University

300 Pasteur Drive, H2200

Stanford, CA 94305, USA

Phone: +1 650 725 4711

Fax: +1 650 498 5047

aiagaru@stanford.edu

Manuscript type: Original article

Word Count: 4918

Clinicaltrials.gov Identifier: NCT03113617 (⁶⁸Ga-RM2), NCT02678351 (⁶⁸Ga-PSMA11)

Running Title: ⁶⁸Ga-RM2 PET in Primary Prostate Cancer

Funding: The study was partially supported by GE Healthcare.

Conflicts of interest/Competing interests: All authors declare that they have no conflict or competing of interest.

Abstract

Rationale: ^{68}Ga -RM2 targets gastrin-releasing peptide receptors (GRPR), which are overexpressed in prostate cancer (PC). Here, we compared pre-operative ^{68}Ga -RM2 PET to post-surgery histopathology in patients with newly diagnosed intermediate- or high-risk PC.

Methods: Forty-one men, 64.0 ± 6.7 -year-old, were prospectively enrolled. PET images were acquired 42 – 72 (median \pm SD 52.5 ± 6.5) minutes after injection of 118.4 – 247.9 (median \pm SD 138.0 ± 22.2) MBq of ^{68}Ga -RM2. PET findings were compared to pre-operative mpMRI ($n=36$) and ^{68}Ga -PSMA11 PET ($n=17$) and correlated to post-prostatectomy whole-mount histopathology ($n=32$) and time to biochemical recurrence. Nine participants decided to undergo radiation therapy after study enrollment.

Results: All participants had intermediate ($n=17$) or high-risk ($n=24$) PC and were scheduled for prostatectomy. Prostate specific antigen (PSA) was 8.8 ± 77.4 (range 2.5 – 504) ng/mL, and 7.6 ± 5.3 (range 2.5 – 28.0) ng/mL when excluding participants who ultimately underwent radiation treatment. Pre-operative ^{68}Ga -RM2 PET identified 70 intraprostatic foci of uptake in 40/41 patients. Post-prostatectomy histopathology was available in 32 patients in which ^{68}Ga -RM2 PET identified 50/54 intraprostatic lesions (detection rate = 93%). ^{68}Ga -RM2 uptake was recorded in 19 non-enlarged pelvic lymph nodes in 6 patients. Pathology confirmed lymph node metastases in 16 lesions, and follow-up imaging confirmed nodal metastases in 2 lesions. ^{68}Ga -PSMA11 and ^{68}Ga -RM2 PET identified 27 and 26 intraprostatic lesions, respectively, and 5 pelvic lymph nodes each in 17 patients. Concordance between ^{68}Ga -RM2 and ^{68}Ga -PSMA11 PET was found in 18 prostatic lesions in 11 patients, and 4 lymph nodes in 2 patients. Non-congruent findings were observed in 6 patients (intraprostatic lesions in 4 patients and nodal lesions in 2 patients). Both ^{68}Ga -RM2 and ^{68}Ga -PSMA11 had higher sensitivity and accuracy rates with 98%, 89%, and 95%, 89%, respectively, compared to mpMRI at 77% and 77%. Specificity was highest for mpMRI with 75% followed by ^{68}Ga -PSMA11 (67%), and ^{68}Ga -RM2 (65%).

Conclusion: ^{68}Ga -RM2 PET accurately detects intermediate- and high-risk primary PC with a detection rate of 93%. In addition, it showed significantly higher specificity and accuracy compared to mpMRI and similar performance to ^{68}Ga -PSMA11 PET. These findings need to be confirmed in larger studies to identify which patients will benefit from one or the other or both radiopharmaceuticals.

Key words: ^{68}Ga -RM2; ^{68}Ga -PSMA11; PET; Prostate Cancer; Histopathology

Introduction

Prostate cancer (PC) remains the most-common non-cutaneous cancer in American men and the second highest cause of cancer-related mortality (1). Cancer stage at diagnosis defines subsequent management. While low-risk PC (Gleason score 6, pre-treatment prostate specific antigen [PSA] <10 ng/mL, and clinical stage T1–T2a) may be managed with active surveillance, patients with higher grade, clinically significant cancers typically receive treatment. Imaging plays a crucial role in initial staging. Multiparametric magnetic resonance imaging (mpMRI) is widely used for initial evaluation. However, mpMRI may miss clinically significant PC in 5-8% (2) to 35% (3) of cases.

Molecular imaging with positron emission tomography and computed tomography (PET/CT) or PET/MRI is changing the landscape of PC staging with the development and regulatory approval of new radiopharmaceuticals. The most promising radiopharmaceuticals target prostate-specific membrane antigen (PSMA). PSMA is highly overexpressed in 90-95% of PC (4-7). However, it is not specific to PC (8,9) and false positive (FP) findings have been reported (10-13). Thus, there is a continued need for other imaging targets. ⁶⁸Ga-RM2 is a bombesin receptor antagonist that targets the gastrin-releasing peptide receptor (GRPR) with high affinity (14). GRPR is highly overexpressed in several cancers including breast (15,16), small cell lung cancer (17), gastrointestinal stromal and neuroendocrine tumors (18,19) and in PC (20-24), especially in earlier stages, making it an attractive target for initial staging (20).

In this study we compared pre-operative ⁶⁸Ga-RM2 PET and mpMRI to histopathology after radical prostatectomy (RP) in patients with newly diagnosed intermediate- or high-risk PC. In a subgroup of patients, comparison with ⁶⁸Ga-PSMA11 PET was also available.

Materials And Methods

Participants

Patients scheduled to undergo RP for newly diagnosed, non-treated, intermediate- or high-risk PC were prospectively enrolled in 2 clinical trials evaluating the performance of ^{68}Ga -RM2 (NCT03113617) and ^{68}Ga -PSMA11 (NCT02678351). This study was approved by the local institutional review board. Written informed consent was obtained from all participants. Pre-surgical clinical assessments included serum PSA, Gleason score, clinical stage, and risk assessment according to the D'Amico classification (25). Patients were followed-up to evaluate time to biochemical recurrence (BCR).

Scanning protocols

^{68}Ga -RM2 PET

Discovery 690 PET/CT ($n=19$), Discovery MI PET/CT ($n=19$) or SIGNA PET/MRI ($n=3$) scanners (GE Healthcare, Waukesha, WI, USA) were used. Details of PET/CT and PET/MRI acquisitions were previously described (26,27). The choice of PET/CT or PET/MRI was dictated by the funding available to support the clinical trials. Discovery MI PET/CT and SIGNA PET/MRI use the same SiPM-based detectors and we previously reported their clinical evaluation (28,29).

^{68}Ga -PSMA11 PET

SIGNA PET/MRI scanner (GE Healthcare, Waukesha, WI, USA) was used. Details of PET/MR image acquisition were previously described (27).

^{68}Ga -RM2 and ^{68}Ga -PSMA11 were synthesized as previously reported (30).

mpMRI protocol

The protocol consisted of T2 weighted imaging (T2WI), diffusion weighted imaging, and dynamic contrast-enhanced imaging sequences using a 3T scanner (MR750, GE Healthcare, Waukesha, WI, USA). Details of mpMR image acquisition were previously described (31).

Histopathology

Hematoxylin-eosin–stained slides from whole-mount prostate specimens were analyzed according to standard of care. The slides were annotated by a genitourinary pathologist (CK) to outline areas of cancer across the entire gland.

Fusion of histology and PET/MRI

The RAPSODI registration framework was used to align corresponding pre-operative axial T2WI, whole-mount histopathology and ^{68}Ga -PSMA11 PET/MRI utilizing rigid, affine, and deformable transformations (32). This registration ensures a slice-to-slice alignment between histology – including ground-truth cancer labels – mpMRI, and PET/MRI. The methodology relies on precise prostate segmentations, automatically generated by a validated deep learning model, and its accuracy was evaluated using a Dice Similarity coefficient (33).

Image analysis

Two nuclear medicine physicians (HD, AI) reviewed and analyzed PET images independently and in a random, blinded fashion, however aware that participants were scheduled to undergo RP for known PC. Any focal uptake of ^{68}Ga -RM2 or ^{68}Ga -PSMA11 higher than the adjacent background and not associated with physiologic accumulation was deemed suspicious for PC (34,35). The number and location of each lesion and its maximum standardized uptake value (SUV_{max}) was recorded. A visual comparison was performed between annotated suspicious lesions on PET and ‘cancer’ annotated histology slides. A lesion was deemed true positive (TP) when annotations on PET and histopathology matched and considered true negative (TN) when uptake on PET was not above background and when there was no ‘cancer’ annotation on corresponding histopathology slide.

mpMRI were interpreted as standard of care using PI-RADS criteria version 2 (36). Lesions with PI-RADS score ≥ 3 were recorded. A PI-RADS score of 3 was considered equivocal, PI-RADS 4 likely, and 5 highly likely for PC.

Statistical analysis

A logistic regression model was used to determine the predictive value of pre-operative biopsy, mpMRI, ^{68}Ga -RM2, and ^{68}Ga -PSMA11 PET for final histopathology and risk prediction. Sensitivity, specificity, and accuracy were stratified to intermediate- and high-risk groups for ^{68}Ga -RM2 and ^{68}Ga -PSMA11. McNemar test determined difference between ^{68}Ga -RM2 and mpMRI for sensitivity, specificity, and accuracy. A Wilcoxon signed-rank test was performed to determine differences between SUV_{max} . Concordance correlation was used for ^{68}Ga -RM2 and ^{68}Ga -PSMA11 SUV_{max} . The degrees of correlation are: >0.99 almost perfect, $0.95 - 0.99$ substantial, $0.90 - 0.95$ moderate, and <0.90 , poor agreement. Spearman correlation was used for evaluation of SUV_{max} and time to BCR. Statistical analyses were performed with Stata v16.1 (Stata Corp LLC College Station, TX, USA). Continuous data are presented as median \pm standard deviation (SD), minimum (min) – maximum (max) values. A *P*-value of <0.05 was considered significant except when Bonferroni correction was applied for concordance analyses (*P*-value <0.0025 significant), and risk prediction (*P*-value <0.017 significant).

Results

Forty-one men, 64.0 ± 6.7 (range 50–78) year-old, scheduled to undergo RP for PC were prospectively enrolled. Seventeen (41.5%) participants had intermediate-risk and 24 (58.5%) had high-risk PC. PSA was 8.8 ± 77.4 (range 2.5–504) ng/mL, and 7.6 ± 5.3 (range 2.5–28.0) ng/mL when excluding participants who received radiation therapy (RT). PSA was undetectable 3 months after RP in all but 3 patients. In one patient, preoperative biopsy was not available and

PC was diagnosed by imaging and PSA. All participants ($n=41$) were imaged with ^{68}Ga -RM2 PET, 36/41 had additional mpMRI, and 17/41 ^{68}Ga -PSMA11 PET. Of these 41 patients, 32 underwent RP and 9 opted for RT after enrollment in the protocol and completion of the scan. Patient characteristics are shown in Table 1.

^{68}Ga -RM2 PET

^{68}Ga -RM2 PET identified 70 intraprostatic foci in 40/41 and focal uptake in 19 non-enlarged pelvic lymph nodes in 6/41 patients. One participant had a negative ^{68}Ga -RM2 PET scan.

In the 32 patients who underwent RP, ^{68}Ga -RM2 identified 54 intraprostatic foci, with 50/54 (92.6%) confirmed by histology (example showed in Figure 1). Four lesions in 4 patients were false negatives (FN). A total of 527 lymph nodes were removed of which 26/527 proved to be metastases in 8 participants. ^{68}Ga -RM2 PET identified 19 lymph nodes in 6 patients, of which 16 were verified by pathology. The 3 unverified positive lymph nodes were seen in the 3 patients whose PSA did not decrease after RP, suggesting TP for metastases. Two lesions were subsequently confirmed by standard of care ^{18}F -Fluciclovine PET after RP.

SUV_{max} of histologically verified intraprostatic lesions was statistically significantly higher than verified lymph node metastases ($P=0.04$) and benign prostatic uptake ($P<0.001$). ^{68}Ga -RM2 uptake in lymph node metastases was also significantly higher than benign nodes ($P<0.001$). SUV_{max} findings are summarized in Table 2.

mpMRI

mpMRI identified lesions in 36/41 participants: 43 PI-RADS ≥ 4 lesions (vs. 64 on corresponding ^{68}Ga -RM2) in 33, and 6 PI-RADS 3 lesions (vs. 5 on corresponding ^{68}Ga -RM2) in 3 patients. In the 30 participants who underwent RP, mpMRI detected 42 intraprostatic lesions with 38 confirmed by histopathology (vs. 50 seen and 48 verified lesions on corresponding ^{68}Ga -

RM2). One suspicious pelvic lymph node was seen and verified as PC metastasis on mpMRI (vs. 18 seen and 16 verified pelvic lymph nodes on corresponding ^{68}Ga -RM2 PET). Four lesions were FP on histopathology while 10 lesions were FN. Table 3 summarizes detection rates of the 3 modalities.

^{68}Ga -PSMA11 and ^{68}Ga -RM2 PET

In 17 participants, ^{68}Ga -RM2 and ^{68}Ga -PSMA11 PET identified 27 and 26 intraprostatic lesions, respectively, and 5 positive pelvic lymph nodes each. Concordance was seen in 18 intraprostatic lesions (example showed in Figure 2) and 3 lymph nodes. Histopathology was available in 13 patients and confirmed 18/19 and 17/18 intraprostatic lesions, and 4/5 and 3/5 lymph node metastases for ^{68}Ga -RM2 and ^{68}Ga -PSMA11, respectively. On a per lesion analysis, ^{68}Ga -RM2 had 1 FP and 2 FN intraprostatic lesions, while ^{68}Ga -PSMA11 had 1 FP and 3 FN. Six patients had incongruent uptake (examples showed in Supplemental Figures 1 and 2): cancer was present in 5/6 lesions on ^{68}Ga -RM2 vs. 3/4 on ^{68}Ga -PSMA11.

^{68}Ga -PSMA11 SUV_{max} of verified PC was significantly higher than lymph node metastases ($P=0.002$). No statistically significant difference where noted when comparing SUV_{max} for ^{68}Ga -RM2 to ^{68}Ga -PSMA11 for intraprostatic cancers ($P=0.43$) or lymph node metastases ($P=0.25$). ^{68}Ga -RM2 and ^{68}Ga -PSMA11 were poorly correlated between the left and right prostate. Table 4 summarizes ^{68}Ga -RM2 and ^{68}Ga -PSMA11 findings.

Sensitivity, specificity, and accuracy

All 3 modalities, ^{68}Ga -RM2, ^{68}Ga -PSMA11 PET and mpMRI, were significant predictors for PC ($P\leq 0.0025$). For intraprostatic lesions, both ^{68}Ga -RM2 and ^{68}Ga -PSMA11 had higher sensitivity and accuracy rates than mpMRI while specificity was highest for mpMRI (Supplemental Table 1). For intraprostatic and lymph node lesions, specificity increased for both radiopharmaceuticals while sensitivity decreased for ^{68}Ga -PSMA11 (Supplemental Table 2).

Significantly higher sensitivity ($P=0.01$) and accuracy ($P<0.01$) were seen for ^{68}Ga -RM2 PET compared to mpMRI.

Sensitivity, specificity, and accuracy for ^{68}Ga -RM2 were slightly higher for high-risk than the intermediate-risk group. For ^{68}Ga -PSMA11, the opposite was found (Supplemental Table 3).

For the relationship and predictive value of PSA (grouped into <5 , 5-10, 10.1-15 and ≥ 15 ng/mL), PI-RADS (3, ≥ 4), and SUV_{max} for histopathological outcome, the only significance found was a higher SUV_{max} of ^{68}Ga -RM2 in PSA ≥ 5 vs. PSA <5 ($P<0.0025$, Figure 3).

Follow-up

Six patients were lost in follow-up. Post-RP, patients ($n=26$) were followed for 28.6 ± 11.7 (range 7.0–47.3) months. PSA remained undetectable in 15 patients, while 11 developed BCR 17.7 ± 10.8 (range 2.8–32.0) months after RP. ^{68}Ga -RM2 SUV_{max} of intraprostatic lesions and time to BCR were negatively correlated ($r=-0.34$), meaning the lower the SUV_{max} , the longer the time to BCR. The correlation of PSA and time to BCR was also negatively correlated ($r=-0.25$), indicating the lower the PSA, the longer the time to BCR.

Discussion

In this study, we prospectively compared GRPR-targeting ^{68}Ga -RM2 PET with whole-mount histopathology after RP in patients with newly diagnosed PC. Sensitivity and accuracy were high for ^{68}Ga -RM2 at 98% and 89%, respectively, and were comparable to ^{68}Ga -PSMA11, and superior to mpMRI. However, specificity of 65% was lower than mpMRI. These results were comparable to previously reported sensitivity, specificity, and accuracy rates of 89%, 81% and 83% for prostate lesions, and sensitivity of 70% for lymph node metastases for ^{68}Ga -RM2 PET/CT in a smaller cohort of 14 men with primary PC and 3 with BCR (37).

^{68}Ga -RM2 and ^{68}Ga -PSMA11 both showed high detection rates for primary PC and lymph

node metastases but were poorly correlated to each other. A recently published study compared ^{68}Ga -RM2 and ^{68}Ga -PSMA11 PET/MRI in staging of 19 men with biopsy proven high-risk PC whereas histopathology was available in 12 patients. While the detection rate of 95% for the primary tumor is similar to our study, the positivity rates for lymph nodes were lower (37% for ^{68}Ga -PSMA11, 21% for ^{68}Ga -RM2). Apart from a negative ^{68}Ga -RM2 in 1 participant, concordant uptake was seen between ^{68}Ga -RM2 and ^{68}Ga -PSMA11 (38). The incongruent uptake pattern in our cohort might be due to our more heterogenous groups of intermediate- and high-risk PC. However, the difference in expression pattern of PSMA and GRPR is consistent with our previous findings in BCR PC (30,39) and is supported by immunohistochemistry showing that GRPR and PSMA expression are not correlated (40). Fassbender et al found in a voxel-based approach that ^{68}Ga -RM2 and ^{68}Ga -PSMA11 in 8 patients with primary PC showed similar averaged SUV_{mean} but, on a per patient basis, different intensity, revealing again a different expression pattern of GRPR and PSMA (41).

We found no correlation between ^{68}Ga -RM2 uptake and Gleason score or tumor volume, but a positive correlation between PSA and ^{68}Ga -RM2 SUV_{max} . SUV_{max} was also negatively correlated to time to BCR. This is supported by previous findings in patients with BCR PC showing a positive correlation between ^{68}Ga -RM2 positivity and PSA and PSA velocity and conversely, a negative correlation of SUV_{max} and PSA with time to BCR indicating the higher ^{68}Ga -RM2 SUV_{max} and PSA, the shorter the time to BCR (27). However, there is controversy (24) as to whether GRPR density is related to a better prognosis of PC (20,21) or found in high-risk tumors as our results indicate. Larger studies with longer follow-up are needed to understand these possible correlations.

The need now is to understand if and how these radiopharmaceuticals may provide complementary and useful information in patients with PC at various stages and risks. Given the high tumor heterogeneity in PC, and that neither ^{68}Ga -RM2 nor ^{68}Ga -PSMA11 are 100% sensitive

or specific and hence attributing to FP and FN lesions, a bispecific tracer that targets GRPR and PSMA simultaneously may present a promising imaging option (42).

Limitations of this study include the relatively small number of patients, especially of participants undergoing both ^{68}Ga -RM2 and ^{68}Ga -PSMA11 PET, and the different imaging modalities used, i.e., different PET/CT scanners and PET/MRI. In addition, not all participants had histopathology data since some elected to undergo RT. Correlating lymph node positivity to histopathology is a challenge as not all lymph nodes seen on PET were resected. PET data were analyzed by readers who were aware that participants were scheduled to undergo RP for known PC, while readers for mpMRI were unaware that participants were scheduled for RP as mpMRI was part of clinical care for PC diagnosis.

Conclusion

^{68}Ga -RM2 PET accurately detects intermediate- and high-risk primary PC with significantly higher specificity and accuracy compared to mpMRI and similar performance to ^{68}Ga -PSMA11 PET. The poor correlation between ^{68}Ga -RM2 and ^{68}Ga -PSMA11 underline the different expression patterns of GRPR and PSMA and the complex tumor biology of PC. Larger prospective studies are needed to identify which patients will benefit from one or the other or both radiopharmaceuticals.

Financial Disclosure

The study was partially supported by GE Healthcare.

Disclaimer

All authors declare that they have no conflict of interest.

Key Points

QUESTION: Is ^{68}Ga -RM2 PET a useful tool in initial staging of PC?

PERTINENT FINDINGS: 41 patients with newly diagnosed PC underwent ^{68}Ga -RM2 PET, a subgroup also had mpMRI ($n=36$) and ^{68}Ga -PSMA11 PET ($n=17$). ^{68}Ga -RM2 PET showed high sensitivity, accuracy, and detection rates of 98%, 89%, and 93%, respectively. Specificity at 65% was lower than mpMRI (75%). Poor correlation to ^{68}Ga -PSMA11 indicate the different expression patterns of GRPR and PSMA in PC.

IMPLICATIONS FOR PATIENT CARE: ^{68}Ga -RM2 PET accurately detected intermediate- and high-risk primary PC with significantly higher sensitivity and accuracy compared to mpMRI and similar performance to ^{68}Ga -PSMA11 PET. Larger prospective studies are needed to identify which patients will benefit from one or the other or both radiopharmaceuticals.

References

1. Siegel RL, Miller KD, Fuchs HE, Jemal A. Cancer Statistics, 2021. *CA Cancer J Clin.* 2021;71:7-33.
2. Rouviere O, Puech P, Renard-Penna R, et al. Use of prostate systematic and targeted biopsy on the basis of multiparametric MRI in biopsy-naive patients (MRI-FIRST): a prospective, multicentre, paired diagnostic study. *Lancet Oncol.* 2019;20:100-109.
3. Johnson DC, Raman SS, Mirak SA, et al. Detection of Individual Prostate Cancer Foci via Multiparametric Magnetic Resonance Imaging. *Eur Urol.* 2019;75:712-720.
4. Bostwick DG, Pacelli A, Blute M, Roche P, Murphy GP. Prostate specific membrane antigen expression in prostatic intraepithelial neoplasia and adenocarcinoma: a study of 184 cases. *Cancer.* 1998;82:2256-2261.
5. Mannweiler S, Amersdorfer P, Trajanoski S, Terrett JA, King D, Mehes G. Heterogeneity of prostate-specific membrane antigen (PSMA) expression in prostate carcinoma with distant metastasis. *Pathol Oncol Res.* 2009;15:167-172.
6. Budaus L, Leyh-Bannurah SR, Salomon G, et al. Initial Experience of (68)Ga-PSMA PET/CT Imaging in High-risk Prostate Cancer Patients Prior to Radical Prostatectomy. *Eur Urol.* 2016;69:393-396.
7. Maurer T, Gschwend JE, Rauscher I, et al. Diagnostic Efficacy of (68)Gallium-PSMA Positron Emission Tomography Compared to Conventional Imaging for Lymph Node Staging of

130 Consecutive Patients with Intermediate to High Risk Prostate Cancer. *J Urol*. 2016;195:1436-1443.

8. Sathekge M, Lengana T, Modiselle M, et al. (68)Ga-PSMA-HBED-CC PET imaging in breast carcinoma patients. *Eur J Nucl Med Mol Imaging*. 2017;44:689-694.

9. Patel D, Loh H, Le K, Stevanovic A, Mansberg R. Incidental Detection of Hepatocellular Carcinoma on 68Ga-Labeled Prostate-Specific Membrane Antigen PET/CT. *Clin Nucl Med*. 2017;42:881-884.

10. Demirkol MO, Kiremit MC, Acar O, Sag AA, Kapran Y. False-Positive Pancreatic Uptake Detected on 68Ga-PSMA PET/CT: A Priority Changing Incidental Finding While Assessing the Need for a Prostate Biopsy. *Clin Nucl Med*. 2017;42:e475-e477.

11. Sasikumar A, Joy A, Nanabala R, Pillai MR, T AH. 68Ga-PSMA PET/CT False-Positive Tracer Uptake in Paget Disease. *Clin Nucl Med*. 2016;41:e454-455.

12. Noto B, Vrachimis A, Schafers M, Stegger L, Rahbar K. Subacute Stroke Mimicking Cerebral Metastasis in 68Ga-PSMA-HBED-CC PET/CT. *Clin Nucl Med*. 2016;41:e449-451.

13. Hermann RM, Djannatian M, Czech N, Nitsche M. Prostate-Specific Membrane Antigen PET/CT: False-Positive Results due to Sarcoidosis? *Case Rep Oncol*. 2016;9:457-463.

14. Ischia J, Patel O, Shulkes A, Baldwin GS. Gastrin-releasing peptide: different forms, different functions. *Biofactors*. 2009;35:69-75.

15. Stoykow C, Erbes T, Maecke HR, et al. Gastrin-releasing Peptide Receptor Imaging in Breast Cancer Using the Receptor Antagonist (68)Ga-RM2 And PET. *Theranostics*. 2016;6:1641-1650.
16. Dalm SU, Martens JW, Sieuwerts AM, et al. In vitro and in vivo application of radiolabeled gastrin-releasing peptide receptor ligands in breast cancer. *J Nucl Med*. 2015;56:752-757.
17. Mattei J, Achcar RD, Cano CH, et al. Gastrin-releasing peptide receptor expression in lung cancer. *Arch Pathol Lab Med*. 2014;138:98-104.
18. Reubi JC, Korner M, Waser B, Mazzucchelli L, Guillou L. High expression of peptide receptors as a novel target in gastrointestinal stromal tumours. *Eur J Nucl Med Mol Imaging*. 2004;31:803-810.
19. Reubi JC. Peptide receptor expression in GEP-NET. *Virchows Arch*. 2007;451 Suppl 1:S47-50.
20. Korner M, Waser B, Rehmann R, Reubi JC. Early over-expression of GRP receptors in prostatic carcinogenesis. *Prostate*. 2014;74:217-224.
21. Beer M, Montani M, Gerhardt J, et al. Profiling gastrin-releasing peptide receptor in prostate tissues: clinical implications and molecular correlates. *Prostate*. 2012;72:318-325.
22. Markwalder R, Reubi JC. Gastrin-releasing peptide receptors in the human prostate: relation to neoplastic transformation. *Cancer Res*. 1999;59:1152-1159.

- 23.** Wieser G, Mansi R, Grosu AL, et al. Positron emission tomography (PET) imaging of prostate cancer with a gastrin releasing peptide receptor antagonist--from mice to men. *Theranostics*. 2014;4:412-419.
- 24.** Ischia J, Patel O, Bolton D, Shulkes A, Baldwin GS. Expression and function of gastrin-releasing peptide (GRP) in normal and cancerous urological tissues. *BJU Int*. 2014;113 Suppl 2:40-47.
- 25.** D'Amico AV, Whittington R, Malkowicz SB, et al. A multivariable analysis of clinical factors predicting for pathological features associated with local failure after radical prostatectomy for prostate cancer. *Int J Radiat Oncol Biol Phys*. 1994;30:293-302.
- 26.** Song H, Harrison C, Duan H, et al. Prospective Evaluation of (18)F-DCFPyL PET/CT in Biochemically Recurrent Prostate Cancer in an Academic Center: A Focus on Disease Localization and Changes in Management. *J Nucl Med*. 2020;61:546-551.
- 27.** Minamimoto R, Sonni I, Hancock S, et al. Prospective Evaluation of (68)Ga-RM2 PET/MRI in Patients with Biochemical Recurrence of Prostate Cancer and Negative Findings on Conventional Imaging. *J Nucl Med*. 2018;59:803-808.
- 28.** Iagaru A, Mitra E, Minamimoto R, et al. Simultaneous whole-body time-of-flight 18F-FDG PET/MRI: a pilot study comparing SUVmax with PET/CT and assessment of MR image quality. *Clin Nucl Med*. 2015;40:1-8.

- 29.** Baratto L, Park SY, Hatami N, et al. ¹⁸F-FDG silicon photomultiplier PET/CT: A pilot study comparing semi-quantitative measurements with standard PET/CT. *PLoS One*. 2017;12:e0178936.
- 30.** Minamimoto R, Hancock S, Schneider B, et al. Pilot Comparison of (6)(8)Ga-RM2 PET and (6)(8)Ga-PSMA-11 PET in Patients with Biochemically Recurrent Prostate Cancer. *J Nucl Med*. 2016;57:557-562.
- 31.** Sonn GA, Fan RE, Ghanouni P, et al. Prostate Magnetic Resonance Imaging Interpretation Varies Substantially Across Radiologists. *Eur Urol Focus*. 2019;5:592-599.
- 32.** Rusu M, Shao W, Kunder CA, et al. Registration of presurgical MRI and histopathology images from radical prostatectomy via RAPSODI. *Med Phys*. 2020;47:4177-4188.
- 33.** Soerensen SJC, Fan RE, Seetharaman A, et al. Deep Learning Improves Speed and Accuracy of Prostate Gland Segmentations on Magnetic Resonance Imaging for Targeted Biopsy. *J Urol*. 2021;206:604-612.
- 34.** Baratto L, Duan H, Laudicella R, et al. Physiological (68)Ga-RM2 uptake in patients with biochemically recurrent prostate cancer: an atlas of semi-quantitative measurements. *Eur J Nucl Med Mol Imaging*. 2020;47:115-122.
- 35.** Fanti S, Minozzi S, Morigi JJ, et al. Development of standardized image interpretation for ⁶⁸Ga-PSMA PET/CT to detect prostate cancer recurrent lesions. *Eur J Nucl Med Mol Imaging*. 2017;44:1622-1635.

36. Weinreb JC, Barentsz JO, Choyke PL, et al. PI-RADS Prostate Imaging - Reporting and Data System: 2015, Version 2. *Eur Urol.* 2016;69:16-40.
37. Kahkonen E, Jambor I, Kemppainen J, et al. In vivo imaging of prostate cancer using [68Ga]-labeled bombesin analog BAY86-7548. *Clin Cancer Res.* 2013;19:5434-5443.
38. Mapelli P, Ghezzi S, Samanes Gajate AM, et al. (68)Ga-PSMA and (68)Ga-DOTA-RM2 PET/MRI in Recurrent Prostate Cancer: Diagnostic Performance and Association with Clinical and Histopathological Data. *Cancers (Basel).* 2022;14.
39. Baratto L, Song H, Duan H, et al. PSMA- and GRPR-Targeted PET: Results from 50 Patients with Biochemically Recurrent Prostate Cancer. *J Nucl Med.* 2021;62:1545-1549.
40. Touijer KA, Michaud L, Alvarez HAV, et al. Prospective Study of the Radiolabeled GRPR Antagonist BAY86-7548 for Positron Emission Tomography/Computed Tomography Imaging of Newly Diagnosed Prostate Cancer. *Eur Urol Oncol.* 2019;2:166-173.
41. Fassbender TF, Schiller F, Zamboglou C, et al. Voxel-based comparison of [(68)Ga]Ga-RM2-PET/CT and [(68)Ga]Ga-PSMA-11-PET/CT with histopathology for diagnosis of primary prostate cancer. *EJNMMI Res.* 2020;10:62.
42. Mitran B, Varasteh Z, Abouzayed A, et al. Bispecific GRPR-Antagonistic Anti-PSMA/GRPR Heterodimer for PET and SPECT Diagnostic Imaging of Prostate Cancer. *Cancers (Basel).* 2019;11.

Figures:

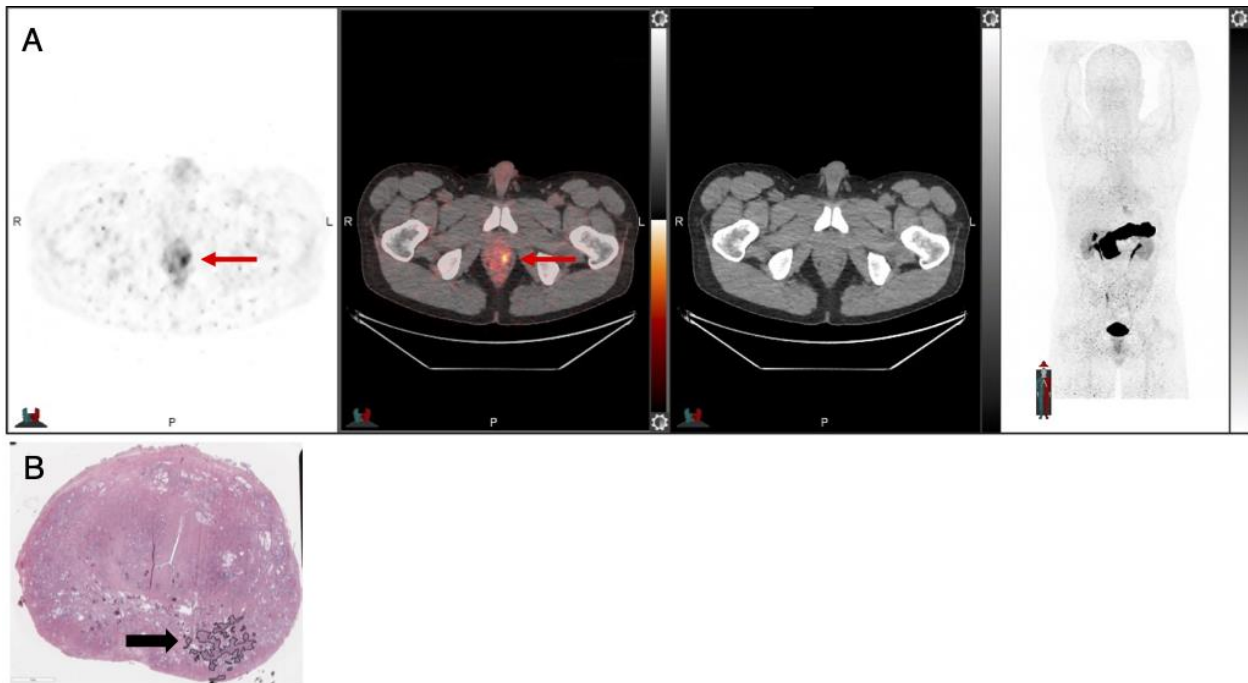


FIGURE 1: 50-year-old patient with intermediate-risk prostate cancer and PSA 5.27 ng/mL. ^{68}Ga -RM2 PET/CT (A, axial PET, fused PET/CT, CT, and maximum intensity projection [MIP] images, respectively) shows focal uptake in the left mid gland (red arrows) correlating to Gleason 4+3 prostate cancer (black arrow) on histology (B).

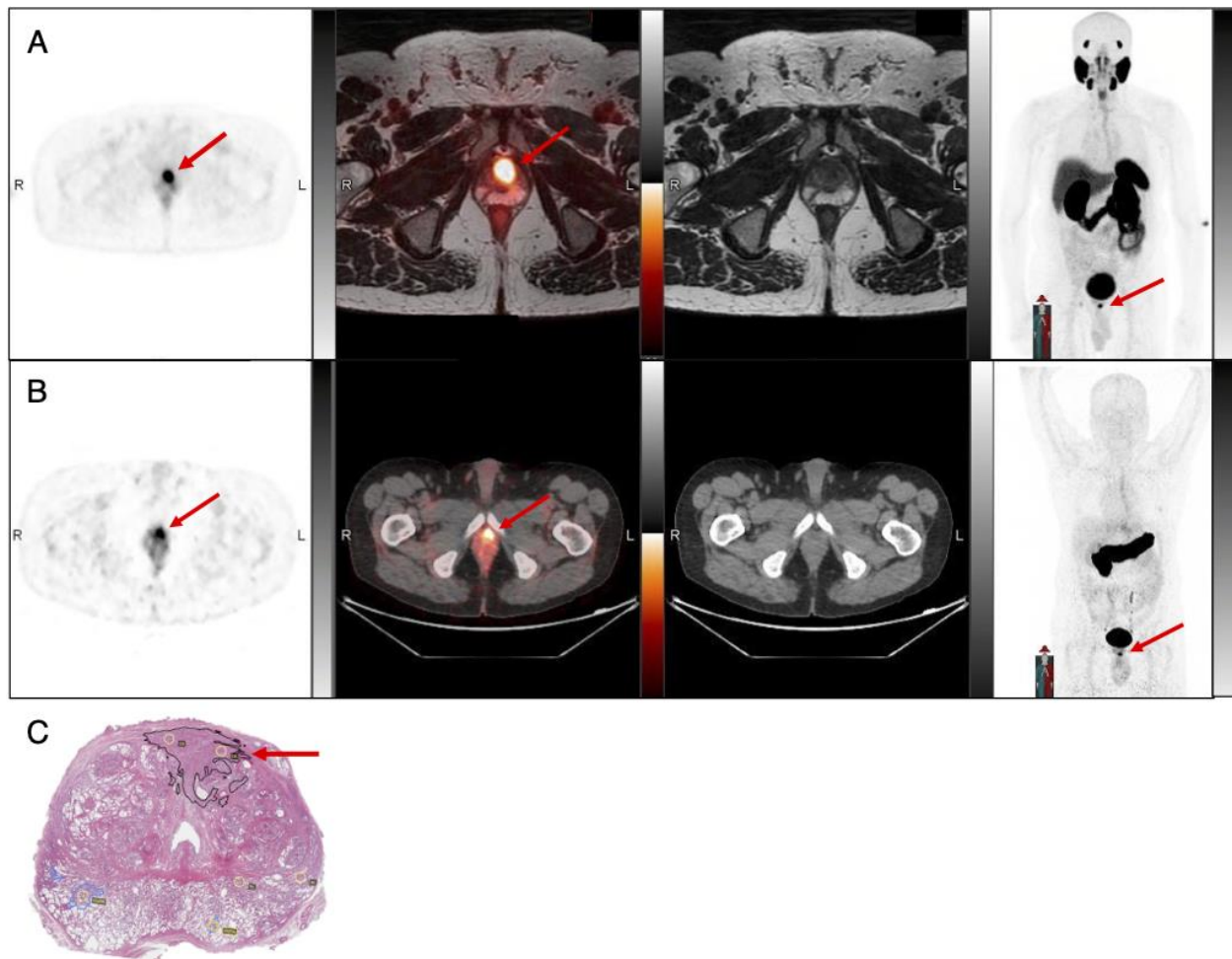


FIGURE 2: 65-year-old man, presenting with PSA 9.5 ng/mL and Gleason 3+4 lesion on pre-surgery biopsy. ^{68}Ga -PSMA11 PET/MRI (A) and ^{68}Ga -RM2 PET/CT (B) axial PET, fused PET/CT, CT, and MIP images, respectively, show concordant focal uptake in the left anterior apex of the prostate (arrows), correlating to Gleason 3+3 on histology (C, arrow).

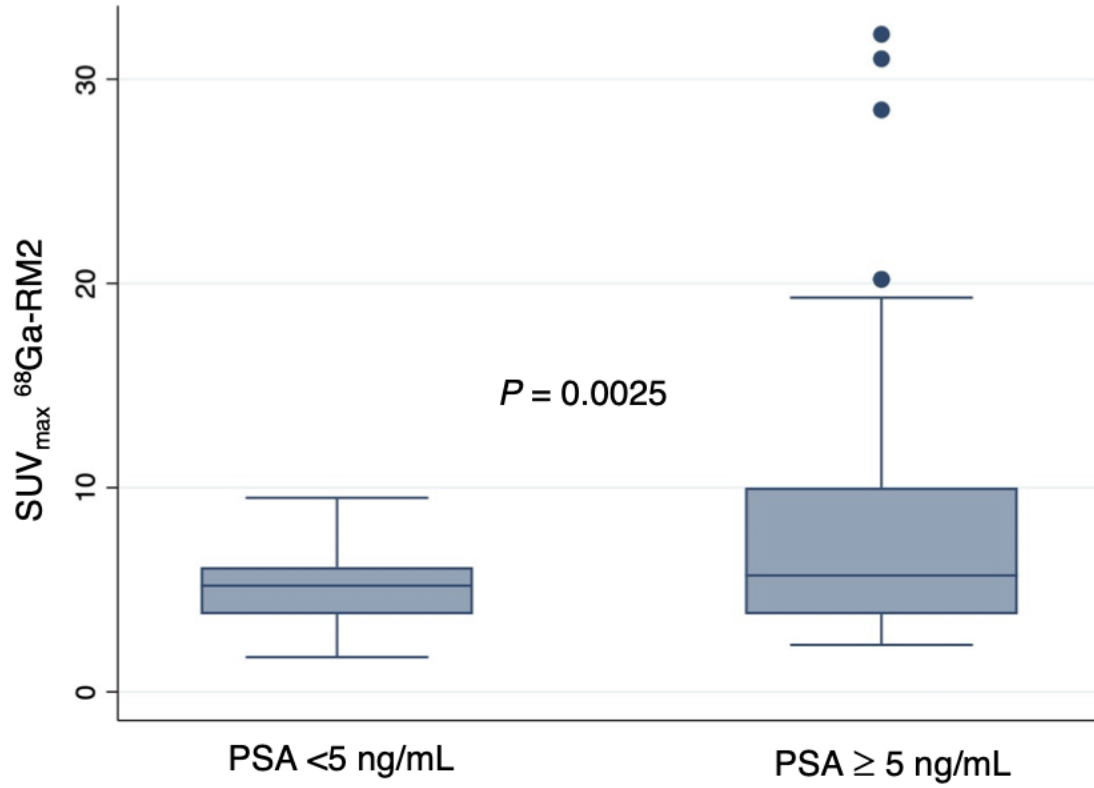


FIGURE 3: Boxplot of $^{68}\text{Ga-RM2}$ SUV_{max} stratified to PSA <5 ng/mL and \geq 5 ng/mL. Patients with PSA \geq 5 ng/mL had a statistically significantly higher SUV_{max} ($P = 0.0025$).

Tables

TABLE 1: Patients' characteristics

<i>N</i>	41		
Age (years)	64 ± 6.7 (50 – 78)		
PSA (ng/ml)	8.8 ± 77.4 (2.5 – 504)		
PSA (excluding radiation therapy patients [ng/ml])	7.6 ± 5.3 (2.5 – 28.0)		
Risk <i>N</i> (%)	Intermediate: 17 (41.5%)		High: 24 (58.5%)
Gleason score from pre-operative biopsy <i>N</i>* (%)	Gleason score 7: 18 (45%)	Gleason score 8: 12 (30%)	Gleason score 9 10 (25%)
Clinical stage <i>N</i> (%)	cT1b: 2 (4.9%) cT1c: 18 (43.9%)	cT2a: 6 (14.6%) cT2b: 6 (14.6%) cT2c: 3 (7.3%)	cT3a: 6 (14.6%)
Pre-operative biopsy available (<i>N</i> patients)	40		
mpMRI (<i>N</i> patients)	36		
⁶⁸Ga-PSMA11 PET (<i>N</i> patients)	17		
Post-operative histopathology available (<i>N</i> patients)	32		

Numerical factors are expressed as median ± standard deviation (range).

*Gleason score of one patient was unavailable.

TABLE 2: SUV_{max} of $^{68}\text{Ga-RM2}$ in verified intraprostatic lesions and lymph node metastases compared to benign prostate and lymph node uptake.

$^{68}\text{Ga-RM2}$	SUV_{max}	<i>P</i> -value
SUV_{max} prostate cancer	6.1 ± 5.9 (2.3 – 32.2)	0.04
SUV_{max} lymph node metastases	4.7 ± 3.3 (1.9 – 12.2)	
SUV_{max} prostate cancer	6.1 ± 5.9 (2.3 – 32.2)	<0.001
SUV_{max} benign prostate	1.8 ± 0.5 (0.5 – 3.3)	
SUV_{max} lymph node metastases	4.7 ± 3.3 (1.9 – 12.2)	<0.001
SUV_{max} benign lymph nodes	0.5 ± 0.2 (0.1 – 0.9)	

Numerical factors are expressed as median \pm standard deviation (range).

TABLE 3: Lesion detection rates with histopathological confirmation amongst modalities.

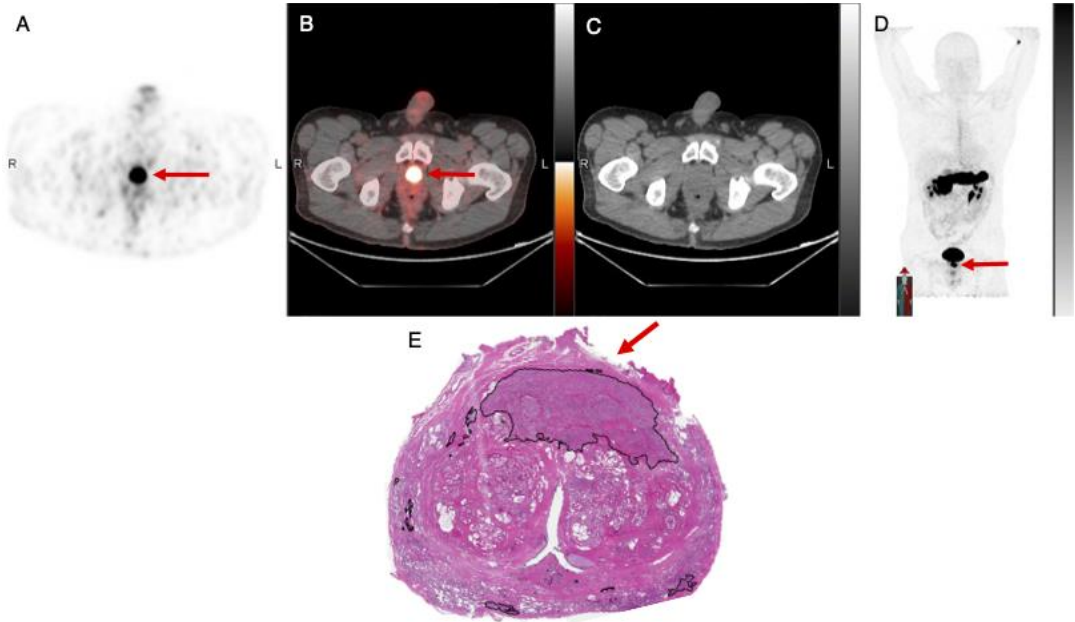
Pre-surgical						Post-surgical whole-mount pathology						
Modality	Prostate lesions	Patient (N)	Lymph nodes	Patient (N)	Negative scan	Prostate lesions (%)	Lymph nodes (%)	FP (N) prostate	FN (N) prostate	FP (N) lymph nodes	FN (N) lymph nodes	Patient (N)
⁶⁸ Ga-RM2	70	40	19	6	1	50/54 (92.5%)	16/19 (88.9%)	4	4	2	1	32
⁶⁸ Ga-PSMA11	26	17	5	4	0	17/18 (94.4%)	4/5 (80%)	1	2	1	1	13
mpMRI	49	36	1	1	2	38/42 (90.5%)	1/1 (100%)	4	10	-	-	30
- PIRADS 3	43	33	-	-	-							
- PIRADS ≥4	6	3	-	-	-							
Biopsy	151	40	-	-	0							
- Gleason score 6	34	16	-	-	0							
- Gleason score ≥7	116	40	-	-	0							

TABLE 4: Correlation of ^{68}Ga -RM2 and ^{68}Ga -PSMA11 PET in 17 patients and comparison to histopathological outcome in 13 patients.

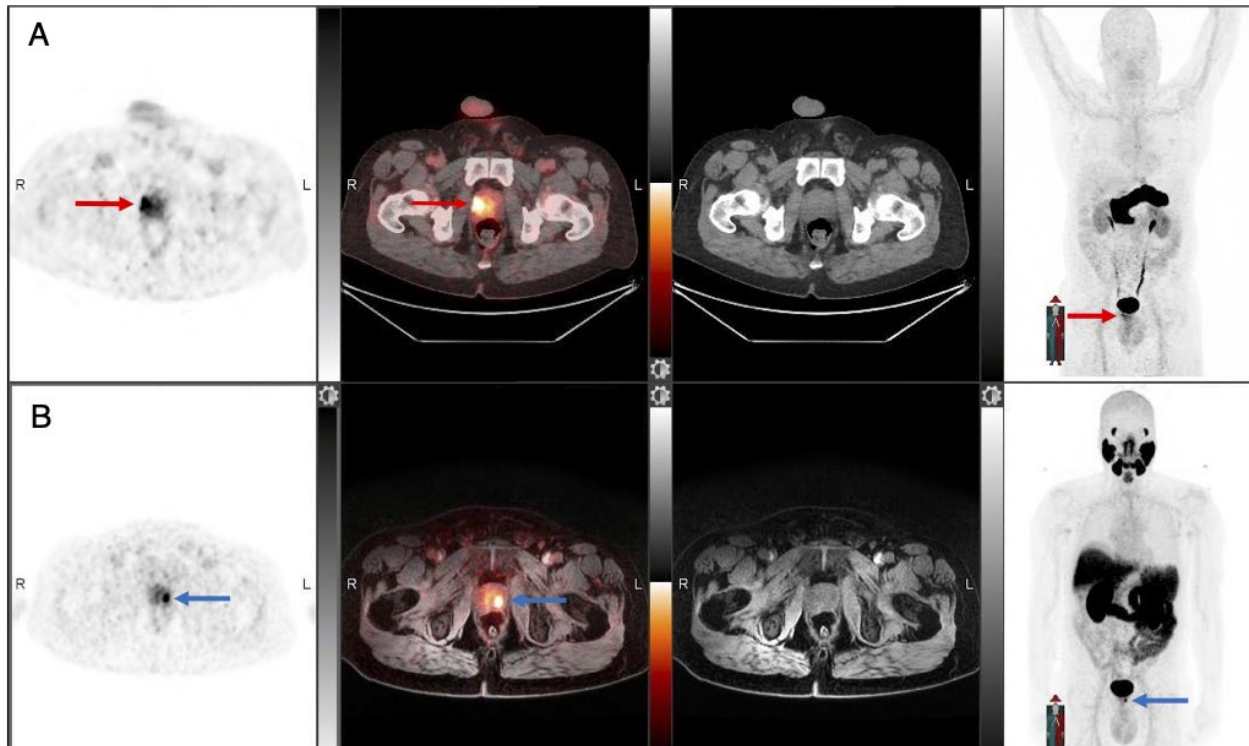
Modality	^{68}Ga -RM2		^{68}Ga -PSMA11		N
Injected activity (MBq)	140.6 ± 11.7 (125.1 – 162.8)		178.7 ± 31.7 (124.3 – 233.8)		17
Time to scan (min)	53.5 ± 7.4 (46 – 72)		48.0 ± 7.4 (40 – 75)		17
Time between ^{68}Ga -RM2 and ^{68}Ga -PSMA11 PET (days)	3.0 ± 5.6 (1 – 21)				17
PSA (ng/mL)	7.5±3.6 (2.5 – 14.7)				17
SUV _{max} prostate lesion (verified)	6.1 ± 4.6 (2.3 – 19.3)	P-value 0.43	7.7 ± 5.8 (3.6 –25.5)		13
SUV _{max} lymph node lesion (verified)	3.9 ± 3.4 (1.9 – 10.7)	P-value 0.25	4.3 ± 1.0 (2.3 – 5.1)		4
Post-surgical pathology	^{68}Ga -RM2		^{68}Ga -PSMA11		
N=13/17	Confirmed/total (%)	FP/FN	Confirmed/total (%)	FP/FN	
Prostate lesions	18/19 (94.7%)	1/2	17/18 (94.4%)	1/3	
Lymph node lesions	4/5 (80%)	1/1	3/5 (60%)	2/2	
Incongruent prostate lesions	5/6 (83%)	1/0	3/4 (75%)	1/0	
Incongruent lymph node lesions	1/1 (100%)	0/2	0/1 (0%)	1/2	
Concordance correlation	Left prostate lesions	95% CI	Right prostate lesions	95% CI	
RM2 vs. PSMA11	0.77	0.56, 0.98	0.68	0.41, 0.95	
Agreement	Poor				

Numerical factors are expressed as median ± standard deviation (range) and as mean (95% confidence interval).

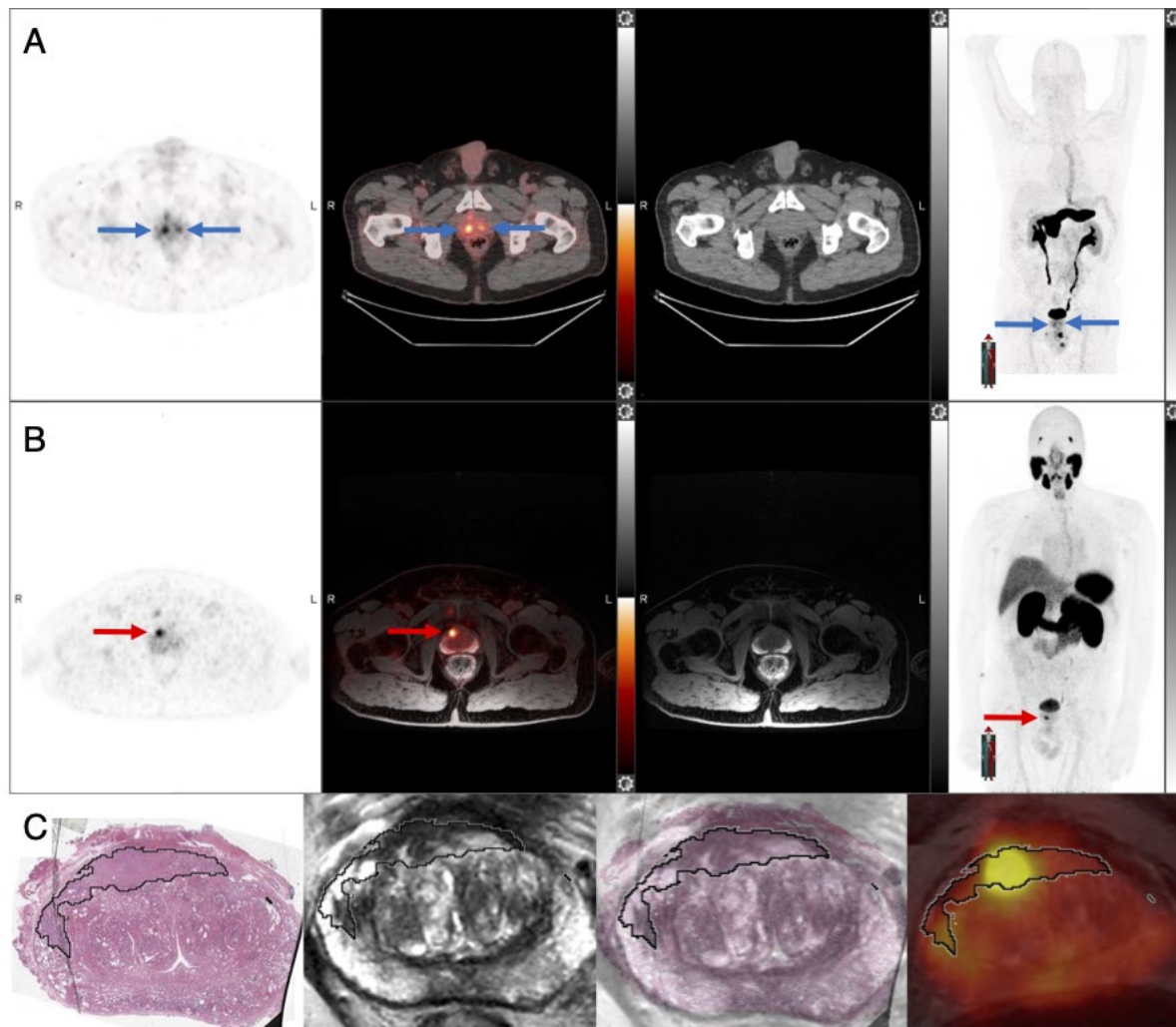
Graphical Abstract



Supplemental Materials



Supplemental Figure 1: 54-year-old patient with intermediate-risk prostate cancer and PSA 5.09 ng/mL. ⁶⁸Ga-RM2 PET/CT (A, axial PET, fused PET/CT, CT, and MIP) shows true positive focal uptake right mid-apex (red arrows) while ⁶⁸Ga-PSMA11 PET/MRI (B) is false negative, and shows false positive uptake mid-apex left of the prostate (blue arrows). Final histopathology demonstrated Gleason score 4+4 prostate adenocarcinoma right mid-apex.



Supplemental Figure 2 64-year-old patient with high-risk prostate cancer and PSA 8.8 ng/mL. ^{68}Ga -RM2 PET/CT (A, axial PET, fused PET/CT, CT, and MIP) shows focal uptake bilateral in the prostate (blue arrows) while ^{68}Ga -PSMA PET/MRI (B) demonstrates uptake right anterior (red arrows). Histology, overlaid with pre-operative axial T2WI and ^{68}Ga -PSMA11 fused PET/MRI (C) showed actual disease expansion crossing the midline to the left side (black outline) correlating to a Gleason score 3+4 prostate adenocarcinoma.

Supplemental Table 1: Sensitivity, specificity, and accuracy (95% confidence interval) of all modalities for prostate cancer localization.

Modality	Sensitivity	Specificity	Accuracy
⁶⁸Ga-RM2	97.9% (88.7, 99.9)	64.7% (38.3, 85.8)	89.1% (78.8, 95.5)
⁶⁸Ga-PSMA11	95.0% (75.1, 99.9)	66.7% (22.3, 95.7)	88.5% (69.8, 97.6)
mpMRI	77.3% (62.2, 88.5)	75.0% (47.6, 92.7)	76.7% (64.0, 86.6)

Supplemental Table 2: Sensitivity, specificity, and accuracy (95% confidence interval) of all modalities for prostate cancer and lymph node metastases localization.

Modality	Sensitivity	Specificity	Accuracy
⁶⁸Ga-RM2	87.1% (76.1, 94.3)	90.8% (81, 96.5)	89% (82.2, 93.8)
⁶⁸Ga-PSMA11	76.7% (57.7, 90.1)	95.5% (77.2, 99.9)	84.6% (71.9, 93.1)
mpMRI	57.6% (44.1, 70.4)	92.9% (82.7, 98.0)	74.8% (65.8, 82.4)

Supplemental Table 3: Sensitivity, specificity, and accuracy (95% confidence interval) for prostate cancer lesions of ⁶⁸Ga-RM2 and ⁶⁸Ga-PSMA11 PET, stratified to participants with intermediate- and high-risk PC.

⁶⁸Ga-RM2	Sensitivity	Specificity	Accuracy
Intermediate-risk	95.5% (77.2, 99.9)	62.5% (24.5, 91.5)	86.7% (69.3, 96.2)
High-risk	100.0% (86.3, 100.0)	66.7% (29.9, 92.5)	91.2% (76.3, 98.1)
⁶⁸Ga-PSMA11			
Intermediate-risk	100.0% (71.5, 100.0)	100.0% (29.2, 100.0)	100.0% (76.8, 100.0)
High-risk	88.9% (51.8, 99.7)	100.0% (29.2, 100.0)	91.7% (61.5, 99.8)